

Formation of the triple-stranded polynucleotide helix, poly(A·A·U)*

[base triplets/poly(A)⁺ mRNA/RNA·DNA binding]

STEVEN L. BROITMAN, DWIGHT D. IM, AND JACQUES R. FRESCO

Department of Biochemical Sciences, Princeton University, Princeton, NJ 08544

Communicated by Donald S. McClure, March 16, 1987

ABSTRACT A polynucleotide helical structure containing two strands of poly(A) and one of poly(U) is reported. As shown by spectroscopic observations, the complex only forms when the poly(A) strands are of M_r between 9000 and 50,000 (degree of polymerization \approx 28–150), whereas the size of the poly(U) strand has no effect. This limitation may explain why poly(A·A·U) was not seen in previous investigations. The potential of the poly(A) tails of mRNA for formation of this triple helix and of A·A·U or/and A·A·T triplet formation to contribute to the binding of specific RNA strands to gene-encoding nucleic acid double helices are noted.

Two types of complexes have been identified in mixtures of poly(A) and poly(U) (1, 2). Poly(A·U) is a right-handed double helix that forms in equimolar mixtures of the interacting homopolymers at neutral pH in aqueous solutions of low or moderate monovalent cation concentration (3–5). Poly(U·A·U) is a three-stranded right-handed helix that forms under similar conditions when the ratio of poly(U)/poly(A) exceeds 1.0 (3, 4, 6, 7). Although these complexes apparently form quite readily, the kinetics of complex formation are not simple, and attainment of the equilibrium structures is relatively slow at room temperature (8). Both the stabilities of these two complexes and the pathways for their thermal dissociation depend upon the cation concentration (6, 7). Comparable deoxynucleotide helices with analogous properties, poly(dA·dT) and poly(dT·dA·dT), have been shown to occur (9). The formation of the hybrid helix poly(U·dA·dT) has also been reported (10). Various spectroscopic and structural features of poly(A·U) and poly(U·A·U) have been extensively investigated (6–8, 11–13). The molecular details of their helical structures have been defined by fiber x-ray diffraction studies (14, 15).

Although the three-stranded complex poly(U·A·U) has been extensively studied, there has been no mention of an analogous helix in which there are two strands of poly(A) and one of poly(U). In this report, we describe the formation and some properties of this complex, poly(A·A·U). This three-stranded structure was initially detected in the course of continuous variation experiments with poly(U) and poly(A₈₆I₁₄), a random copolymer containing 86 mol % A residues and 14 mol % I residues. Poly(A·A·U) was also observed to form when certain preparations of poly(A) were mixed with all preparations of poly(U). In due course, it emerged that poly(A) size is the critical parameter for formation of this particular triple helix.

MATERIALS AND METHODS

Polynucleotides. Poly(U), some poly(A), and oligo(A) [degree of polymerization or number of base residues (dp) = 17–29] were obtained from Pharmacia. Other poly(A) samples and poly(A₈₆I₁₄) were synthesized using polynucleotide

phosphorylase from *Micrococcus luteus* (Pharmacia) (16). All polynucleotides were recovered by lyophilization as the Na⁺ salt after exhaustive dialysis in sequence versus 0.1 M EDTA/1.0 M NaCl, pH 7.0, then versus 1.0 M NaCl, and finally versus deionized water.

Some poly(A) samples were fractionated by gel filtration. Generally, 10–100 mg of poly(A) in 2–10 ml of eluting buffer [0.1 M NaCl/0.001 M cacodylate (Na⁺/H⁺)/0.005 M EDTA, pH 7.0] were applied to a column (2 cm × 50–100 cm) of Sephadex G-50 or G-100 at 4°C. After elution, appropriate fractions were pooled, dialyzed, and lyophilized. Fractions were sized in either of two ways. In one, $s_{20,w}$ was measured in a Spinco model E ultracentrifuge in 0.15 M NaCl/0.001 M cacodylate (Na⁺/H⁺), pH 7.0, and converted to M_r using the sedimentation coefficient versus M_r relations for poly(A) (17) or for poly(U) (18). Alternatively, polymers were sized on polyacrylamide denaturing gels (cf. 19).

High-molecular-weight poly(A) (dp \approx 550) was reduced in size either by *Neurospora crassa* endonuclease (EC 3.1.30.1) (Boehringer Mannheim) or by sonication. For enzymatic digestion, 10 ml of the large polymer, 1–10 mg/ml, was incubated in the standard solvent (see below) at 22°C with 50–500 units of enzyme. Following incubation, the reaction was phenol extracted, and the polymer was recovered after dialysis. For sonication, 10 ml of the large polymer, 1–10 mg/ml, in the standard buffer was placed in a 30-ml round-bottom glass centrifuge tube that was immersed in a salt/ice bath at –2°C. A standard tapered microtip probe of a model W-375 Heat System/Ultrasonics (Farmingdale, NY) sonicator was immersed halfway into the sample solution, which was then sonicated for 5–9 hr (50% pulse time) at intensity setting 4. The sonicate was passed through a Gelman disposable filter of pore size 0.45 μ m. Degradation by either method was monitored at various intervals by PAGE; treatment was stopped when the population of desired size was obtained (e.g., Fig. 1).

Solvents. All experiments were conducted in 0.01 M cacodylate (Na⁺/H⁺)/0.0001 M EDTA/0.15 M NaCl/0.005 M MgCl₂, pH 7.0.

Spectrophotometry. A Cary 14 recording spectrophotometer with a thermoregulated sample compartment was used. Monochromator and photometric accuracy were confirmed using benzene vapor and potassium dichromate standards, respectively. Slit widths were usually maintained at <0.3 mm. Sample and reference cuvettes were thermoregulated by circulating fluid from a constant-temperature bath through jacketed cell holders. Sample temperature was monitored to \pm 0.5°C with a calibrated thermistor probe (Thermometrics, Edison, NJ) inserted in a “dummy” cuvette. Desiccated air was blown through the cell compartments to prevent condensation.

The publication costs of this article were defrayed in part by page charge payment. This article must therefore be hereby marked “advertisement” in accordance with 18 U.S.C. §1734 solely to indicate this fact.

Abbreviation: M_r , relative molecular mass or molecular weight; dp, degree of polymerization or number of base residues.

*This is paper no. 16 in the series “Polynucleotides.” The previous paper in the series is ref. 26.



FIG. 1. Electrophoretic analysis of poly(A) before and after sonication. Polymer samples [200 μ g in 20 μ l of Tris-phosphate-EDTA gel buffer (19) with tracking dye] were applied to 8% polyacrylamide denaturing gels containing 8 M urea. Electrophoresis was done at 22°C, 150 V, and 35 mA for 5 hr. Gels were stained with 0.2% methylene blue. (Lanes 1 and 7) Yeast tRNA_{3^{eu}}, tRNA_{1^{gly}}, and 5S RNA M_r markers; (lane 2) poly(A) (dp \approx 550); (lane 3) poly(A) sonicated 7 hr; (lane 4) poly(A) sonicated 9 hr; (lane 5) poly(A) (dp \approx 120); and (lane 6) oligo(A) (dp = 17–29).

Continuous Variation Titrations. Mixing curve experiments were done as previously described (20–22). Polymers were dissolved in buffer and adjusted to equimolar residue concentrations ($\approx 10^{-4}$ M) using their extinction coefficients (ϵ). Successive mixtures containing varying proportions of the interacting species were prepared using a syringe microburet (model SB2, Micro-Metric Instrument, Cleveland, OH). Mixtures sat at room temperature for 1 hr to promote helix nucleation, and then they were incubated at 4°C for at least 1 week to ensure equilibrium. Absorption spectra were recorded after sufficient equilibration at the desired temperature; spectra were sometimes re-recorded to check that equilibrium at the new temperature was attained.

Thermal Denaturation Experiments. Melting curves were recorded on the Cary 14 spectrophotometer using a modified, highly stable quartz-halogen light source (Aviv Associates, Lakewood, NJ). Instrument stability was additionally enhanced by changing electrical resistors on the preamplifier circuit. Thermoregulation was maintained and monitored as described above. Sample temperature was increased linearly

at $\approx 10^\circ\text{C/hr}$ (slow enough to continually maintain chemical equilibrium) by mechanically changing the thermoregulator setting. Baselines were recorded over the temperature range used.

Circular Dichroism. CD spectra were recorded on a Cary 60 spectropolarimeter. Samples were measured in jacketed quartz cuvettes (with strain-free windows) through which thermoregulated fluid was circulated.

RESULTS

Stoichiometry of Complexes Formed from Interaction of Poly(A) and Poly(U). The stoichiometry of complexes formed was determined from mixing curve titrations observed at various wavelengths. Plots of absorbance versus mole fraction of poly(A) residues showed the expected endpoints at $X_A = 0.33$ and 0.50, corresponding to the three-stranded helix poly(U·A·U) and the double helix poly(A·U), respectively. When monitored at 280 nm, an additional endpoint at $X_A = 0.67$ was observed at 4°C with certain preparations of poly(A) (Fig. 2). This endpoint corresponds to a previously unknown complex with A₂U stoichiometry, poly(A·A·U).

Mixing curve plots over the near ultraviolet range indicate that 280 nm is the wavelength of choice for observing formation of the structure poly(A·A·U)—i.e., $\Delta\epsilon = \{\epsilon \text{ poly(A·A·U)} - [\epsilon \text{ poly(A·U)} + \epsilon \text{ poly(A)}]\}$ is at a maximum. At this wavelength, poly(A·A·U) is sufficiently hyperchromic relative to its poly(A·U) and poly(A) precursors so that careful measurements make its existence unmistakable.

Mixing curves recorded at higher temperatures show the endpoint at $X_A = 0.67$ up to 30°C, but not at 45°C and above (see Fig. 2 data at 45°C). At those higher temperatures there is an endpoint at $X_A = 0.5$ (data not shown) that indicates that at $X_A = 0.67$ there is only a mixture of poly(A·U) and poly(A).

An endpoint corresponding to the poly(A·A·U) type of three-stranded helix was also observed (data not shown) when the copolymer poly(A₈₆,I₁₄) was titrated with poly(U) at 4°C—i.e., a complex containing two copolymer strands and one homopolymer strand such that A·A·U triplets are present.

Isobestic Analysis. When a successive series of mixtures of a mixing curve contain different proportions of the same two components, the spectra of the mixtures may share one or

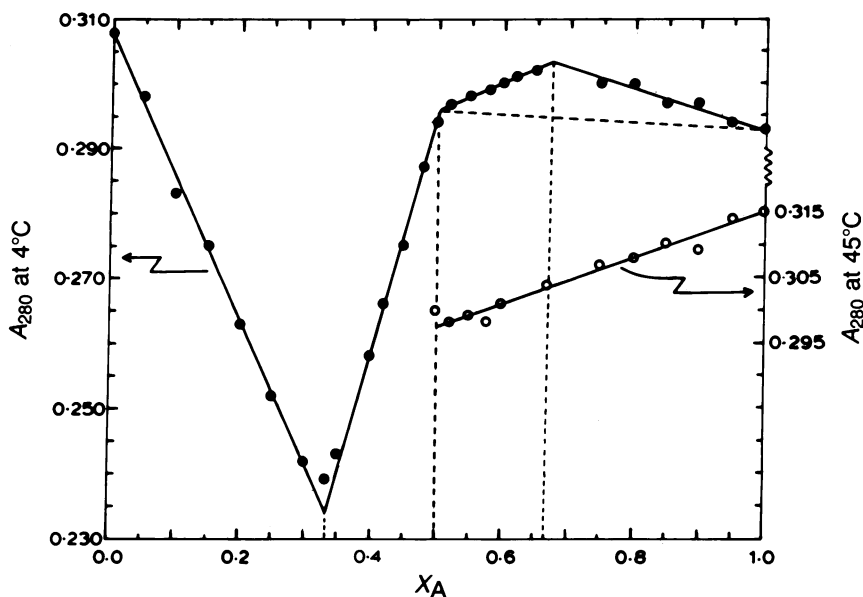


FIG. 2. Mixing curve titration of poly(A) (dp \approx 120) + poly(U) (dp \approx 127) incubated at 4°C to equilibrium. Endpoints were invariant at 20°C and 30°C. At 45°C and 57°C the endpoint at $X_A = 0.67$ was absent. The horizontal dashed line at 4°C indicates absorbance expected if poly(A·A·U) is unformed.

more wavelengths of common extinction coefficient. These spectra will therefore intersect at such a wavelength(s), giving rise to an isosbestic point(s). Each pair of species will give rise to an isosbestic wavelength for those mixtures in which they are both present.

UV absorption spectra of successive mixtures of the mixing curve were superimposed in order to locate the isosbestic wavelength(s). It had previously been observed (6) that the spectra of all mixtures between $X_A = 0.50$ and 1.0 intersect at a single isosbestic point, indicating that these mixtures contain varying proportions of the same two absorbing species, poly(A·U) and poly(A). In the present work, two isosbestic wavelengths were observed in these mixtures at 4°C and 30°C. One (283 nm at 4°C; 282.5 nm at 30°C) was common to the mixtures between $X_A = 0.50$ and 0.67; a distinctly different one (277.5 nm at 4°C; 279 nm at 30°C) was shared by those between $X_A = 0.67$ and 1.0 (Fig. 3). This occurrence of different isosbestic wavelengths indicates the presence of a third structural species [in addition to poly(A·U) and poly(A)], poly(A·A·U). Thus, the mixtures between $X_A = 0.50$ and 0.67 contain poly(A·U) and poly(A·A·U), whereas those between $X_A = 0.67$ and 1.0 contain poly(A·A·U) and poly(A). When the temperature was raised to 45°C, where the mixing curve showed no endpoint for poly(A·A·U), only one isosbestic wavelength (282 nm) was evident for all mixtures between $X_A = 0.5$ and 1.0 (Fig. 3).

This analysis of the location of isosbestic points provides independent confirmation that poly(A·A·U) is a distinct species.

Thermal Denaturation of Poly(A·A·U). The melting of poly(A·A·U) follows a complex course. As evident in Fig. 4, A_{280} is unchanged up to 30°C and then drops sharply between 32°C and 44°C. This first cooperative, hypochromic transition is consistent with the thermal stability range for poly(A·A·U) ascertained from mixing curves at different temperatures. In view of the mixing curve endpoint at $X_A = 0.5$ at 45°C (data not shown), the absence of an endpoint at 0.67 (Fig. 2), and

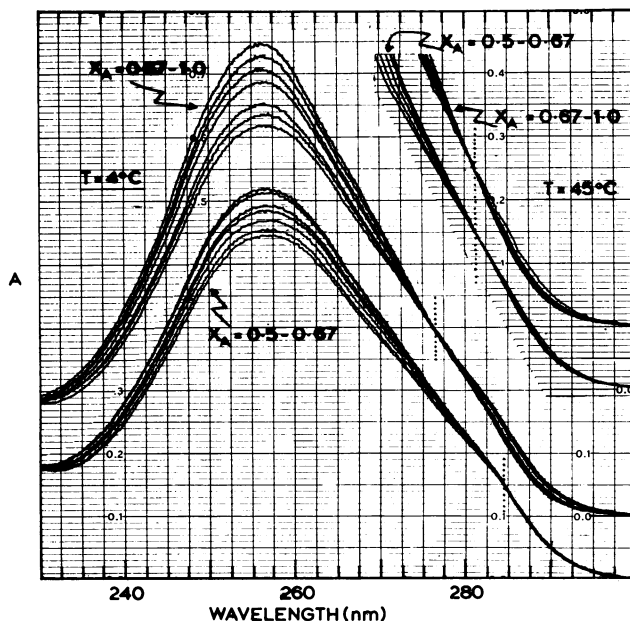


FIG. 3. Isosbestic analysis of sequential mixtures from mixing curve titration of poly(A) ($dp = 120$) and poly(U). The spectra shown between 230 and 300 nm were taken at 4°C, whereas those shown between 270 and 300 nm are of the same mixtures at 45°C. For clarity, the spectra of the two sets of mixtures at both temperatures are displaced on the absorbance scale. Note isosbestic points indicated by vertical dotted lines, two at 4°C, but only one at 45°C.

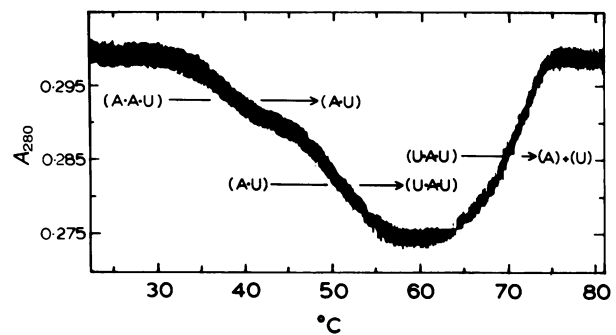


FIG. 4. Melting profile of poly(A·A·U) in the standard solvent. Note the three transitions.

the course of melting above that temperature (described below), it is concluded that this first transition represents the phase transition poly(A·A·U) \rightarrow poly(A·U) + poly(A), with $t_m \approx 38^\circ\text{C}$. This first transition is absent when poly(A·A·U) is not formed in the A_2U mixture (Fig. 9).

The remainder of the melting profile follows the course observed previously (7) for the melting of poly(A·U). This is expected because the melting of single-stranded poly(A), the other component in the mixture, is masked near 280 nm (7). Thus, the melting of poly(A·U) is evident in the A_2U mixture as a second (hypochromic) transition between 45°C–57°C, with $t_m \approx 50^\circ\text{C}$. This transition represents the previously studied (6, 7, 11) “2 \rightarrow 3” disproportionation transition, 2 poly(A·U) \rightarrow poly(U·A·U) + poly(A). It is followed by a third (hyperchromic) transition with $t_m \approx 70^\circ\text{C}$, corresponding to the cooperative melting of poly(U·A·U) to its single strands.

In sum, the thermal melting profile of the A_2U mixture follows a course of denaturation fully consistent with the interpretation that at low temperature this mixture contains poly(A·A·U).

Spectral Properties of Poly(A·A·U). Figs. 5 and 6 show, respectively, CD and absorption spectra of the various complexes formed from the interaction of poly(A) and poly(U). It is apparent that these complexes are distinguishable by both of these properties, with CD being more distinctive. Given the established right-handed chirality of poly(A·U) (5, 14), the similarity of the sign of the CD spectra for poly(A·U) and poly(A·A·U) and the greater intensity of the latter suggest the right-handed chirality of the latter complex as well.

Fig. 7a shows the CD spectrum of poly(A·A·U) at 25°C and for comparison a CD spectrum calculated by summing those for equimolar amounts of poly(A·U) base pairs and poly(A) single-stranded residues in the same solvent and temperature. As expected, the observed and calculated spectra differ significantly, further confirming that the A_2U mixture con-

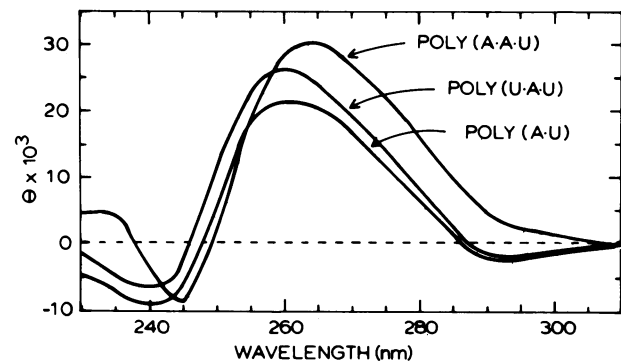


FIG. 5. CD spectra of poly(A·U), poly(U·A·U), and poly(A·A·U) at same total residue concentration, 1.02×10^{-4} M, at 25°C, measured in 1-cm pathlength cells.

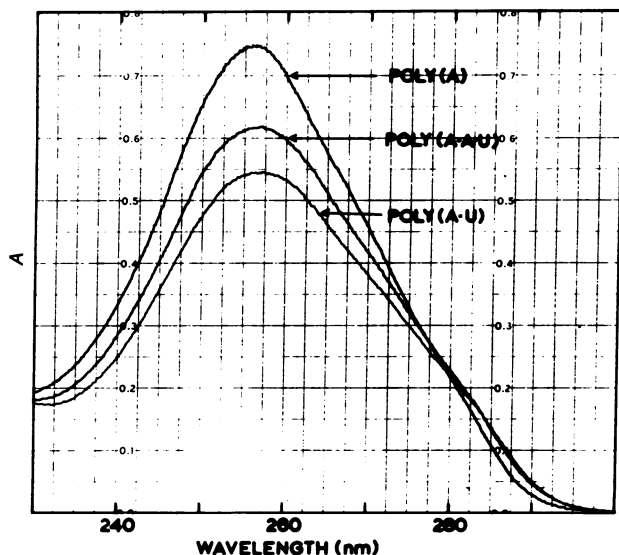


FIG. 6. Absorption spectra of poly(A), poly(A·U), and poly(A·A·U) at same total residue concentration at 4°C. Three isosbestic wavelengths are readily discernible in this figure, the two made evident in Fig. 3 and the additional one due to the intersection at 280 nm of the spectra of poly(A) and poly(A·U).

tains a distinct species at 25°C. However, at 45°C (Fig. 7b), where the first melting transition for poly(A·A·U) is complete, the observed and calculated spectra do superimpose.

The spectral absorbance change accompanying the dissociation of poly(A·A·U) to poly(A·U) + poly(A) between 30°C and 45°C is shown in Fig. 8. This melting spectrum contains two maxima, a hyperchromic one near 262 nm and a hypochromic one near 280 nm. While the change at 262 nm is larger than that at 280 nm, it is not useful for selectively following the melting of poly(A·A·U), as is 280 nm, where the melting of poly(A) does not result in a significant absorbance change. It is worth noting that Fig. 8 also indicates that the melting transition for poly(A·A·U) is masked near 276 nm.

Molecular Weight Effects. Previous studies using the same techniques employed in the present work had given no indication of the formation of poly(A·A·U) (6, 7). In addition, most poly(A) preparations tested for poly(A·A·U) formation during the present study did not form the complex. In an effort to resolve this discrepancy, the effect of poly(A) size was investigated. The original sample of poly(A) observed to form the complex had a weight average $dp \approx 120$; one sample of poly(A) that did not form the complex had a weight average $dp \approx 550$. When the latter was degraded to $dp \approx 30-150$ (Fig. 1), the complex now formed completely, as indicated by

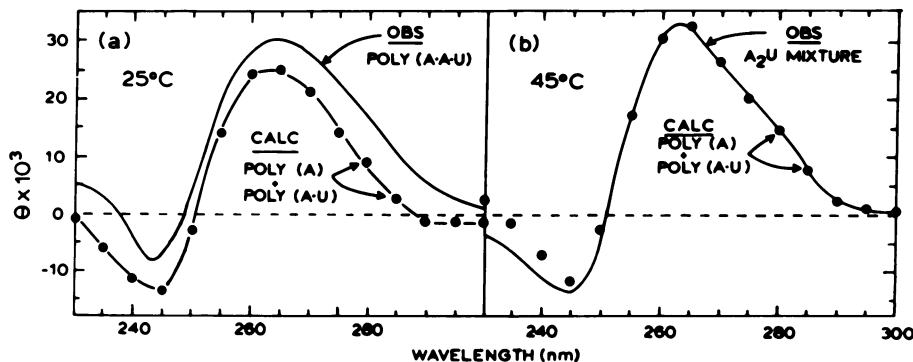


FIG. 7. Comparison of observed (OBS) CD spectrum of poly(A·A·U) and CD spectrum calculated (CALC) for the sum of its components, poly(A·U) and poly(A) at 25°C (a) and 45°C (b). The spectra superimpose at 45°C, where poly(A·A·U) is dissociated into its components, but not at 25°C, where poly(A·A·U) is a distinct stable species.

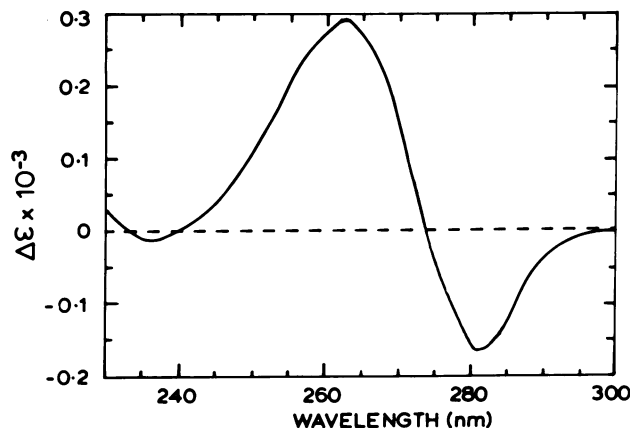


FIG. 8. Denaturation spectrum calculated for the dissociation of poly(A·A·U) \rightarrow poly(A·U) + poly(A) on raising temperature from 30°C to 45°C—i.e., $\Delta\epsilon = [\epsilon 2 \text{ poly(A·U)}/3 + \epsilon \text{ poly(A)}/3]_{45^\circ} - \epsilon \text{ poly(A·A·U)}_{30^\circ}$.

mixing curve endpoints, isosbestic wavelengths, and melting transitions (e.g., Fig. 9). On the other hand, a preparation of oligo(A) with $dp = 17-29$ only formed the complex in low yield; and a re-examination of old plots of mixing curves done with a series of oligoadenylates with $dp = 4-13$ showed that the A_2U complex did not form at all (23). Further, it was found using poly(A) with weight average $dp \approx 120$ that samples of poly(U) ranging in weight average dp from ≈ 100 to 1500 all form the complex. These results show that formation of poly(A·A·U) is limited by the size of the poly(A) strands ($dp \approx 28-150$ under the conditions studied) but is unaffected by the size of the poly(U) strand.

DISCUSSION

Evidence has been presented for the formation of the previously unrecognized three-stranded complex, poly(A·A·U), under physiological solvent and temperature conditions. A possible explanation for the intermediate poly(A) size requirement for poly(A·A·U) formation is that the geometry of the (A·A·U) triplet and/or the third strand backbone suffer increasing deformation as each succeeding residue of the third strand winds around the core double helix. Eventually, the deformation is amplified to the point where third strand binding becomes unfavorable. Smaller poly(A) sizes would be the equivalent to introducing periodic discontinuities in the third strand, thereby relieving the deformation. In that case, the reasons for the failure of very short oligo(A) to also form the triple structure (23) may be that the enthalpy

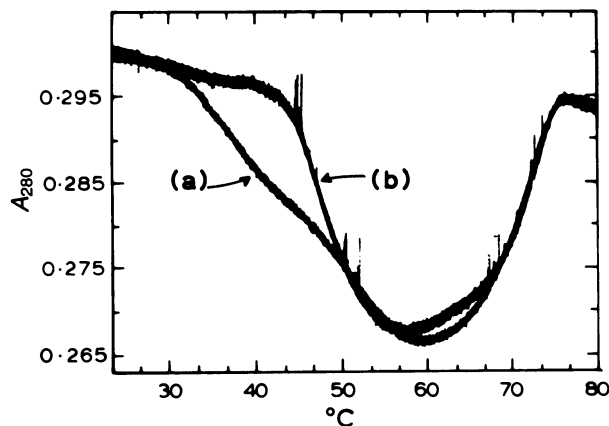


FIG. 9. Comparison of melting profiles of A_2U mixtures prepared with poly(A) before (profile *b*) and after (profile *a*) sonication. The same poly(U) was used in both cases. The two profiles are superimposed. A transition for poly(A·A·U) is only evident after sonication. The same result was obtained when large poly(A) was enzymatically reduced to a similar size.

loss due to "end effects," as well as the entropy of mixing, are prohibitive. It is also conceivable that the much greater configurational entropy of the longer single strands of poly(A), due to their more available degrees of freedom (24), disfavors their association with poly(A·U). A subsequent report will present observations concerning other unusual aspects of the thermodynamics and molecular structure of poly(A·A·U) (S.L.B., D. F. Davis, D.D.I. & J.R.F., unpublished work).

The formation of poly(A·A·U) indicates the potential for A·A·U (and by analogy, A·A·T) triplets under physiological conditions. Such triplets could have a structural or functional role in some type of intra- or intermolecular nucleic acid interaction. For example, formation of a poly(A·A·U) helical segment could constitute a mechanism underlying a physiological role for the poly(A) tails of mRNA, whose size range coincides approximately with that favoring formation of this new complex (25). The observation of the A·A·U triplet in a three-stranded nucleic acid helix also completes the range of base triplet interactions (the others observed in such helices being U·A·T, U·A·U, G·G·C, and C·G·C) required for versatility in third-strand RNA binding to specific target sequences in gene-encoding double helices. Such interaction does not require double helix denaturation and constitutes the basis for a plausible mechanism of gene control at the genomic level (J.R.F., unpublished work).

This work was supported by a grant from the National Science Foundation (DMB 8419060) and a Predoctoral National Research Service Award to S.L.B. from National Institutes of Health Grants 5T 32 GM 07388 and 5T 32 GM 07312. We thank Dr. Robert Naylor of Pharmacia for oligoadenylates and Thermometrics, Inc., Edison, NJ for thermistors.

1. Warner, R. C. (1956) *Fed. Proc. Fed. Am. Soc. Exp. Biol.* **15**, 379.
2. Rich, A. & Davies, D. R. (1956) *J. Am. Chem. Soc.* **78**, 3548.
3. Felsenfeld, G., Davies, D. R. & Rich, A. (1957) *J. Am. Chem. Soc.* **79**, 2023.
4. Felsenfeld, G. & Rich, A. (1957) *Biochim. Biophys. Acta* **26**, 457-468.
5. Fresco, J. R. (1959) *Trans. N.Y. Acad. Sci. Ser. II* **21**, 653-658.
6. Stevens, C. L. & Felsenfeld, G. (1964) *Biopolymers* **2**, 293-314.
7. Blake, R. D., Massoulie, J. & Fresco, J. R. (1967) *J. Mol. Biol.* **30**, 291-308.
8. Blake, R. D. & Fresco, J. R. (1966) *J. Mol. Biol.* **19**, 145-160.
9. Howard, F. B., Frazier, J. & Miles, H. T. (1971) *J. Biol. Chem.* **246**, 7073-7086.
10. Riley, M., Mailing, B. & Chamberlin, M. J. (1966) *J. Mol. Biol.* **20**, 359-389.
11. Miles, H. T. & Frazier, J. (1964) *Biochem. Biophys. Res. Commun.* **14**, 21-28.
12. McDonald, C. C., Phillips, W. D. & Penman, S. (1964) *Science* **144**, 1234-1237.
13. Pan, Y. E. & Bobst, A. M. (1973) *Biopolymers* **12**, 367-371.
14. Arnott, S., Fuller, W., Hodgson, A. & Prutton, I. (1968) *Nature (London)* **220**, 561-564.
15. Arnott, S. & Bond, P. J. (1973) *Nature (London) New Biol.* **244**, 99-101.
16. Heppel, L. A., Ortiz, P. J. & Ochoa, S. (1967) *J. Biol. Chem.* **242**, 695-710.
17. Fresco, J. R. & Doty, P. (1957) *J. Am. Chem. Soc.* **79**, 3928-3929.
18. Richards, E. G., Flessel, C. P. & Fresco, J. R. (1963) *Biopolymers* **1**, 431-446.
19. Maniatis, T., Fritsch, E. F. & Sambrook, J. (1982) *Molecular Cloning: A Laboratory Manual* (Cold Spring Harbor Laboratory, Cold Spring Harbor, NY), pp. 173-185.
20. Job, P. (1928) *Ann. Chim. (Paris)* **9**, 113-134.
21. Felsenfeld, G. (1958) *Biochim. Biophys. Acta* **29**, 133-144.
22. Lomant, A. & Fresco, J. R. (1975) *Prog. Nucleic Acid Res.* **15**, 185-218.
23. Blake, R. D. & Fresco, J. R. (1973) *Biopolymers* **12**, 775-789.
24. Flory, P. (1953) *Principles of Polymer Chemistry* (Cornell Univ. Press, Ithaca, NY), pp. 512-514.
25. Zeevi, M., Nevins, J. R. & Darnell, J. E., Jr. (1981) *Cell* **26**, 39-46.
26. Topal, M. D. & Fresco, J. R. (1974) *Biophys. Chem.* **2**, 193-195.